

Spectroscopic, Redox, and Structural Characterization of the Ni-Labile and Nonlabile Forms of the Acetyl-CoA Synthase Active Site of Carbon Monoxide Dehydrogenase

William K. Russell,[†] Christina M. V. Stålhandske,^{‡,§} Jinqiang Xia,^{†,⊥} Robert A. Scott,[‡] and Paul A. Lindahl^{*,†}

Contribution from the Department of Chemistry, Texas A&M University, College Station, Texas 77843, and Center for Metalloenzyme Studies and Department of Chemistry, University of Georgia, Athens, Georgia 30602-2556

Received April 7, 1998

Abstract: The α subunit of carbon monoxide dehydrogenase from *Clostridium thermoaceticum* was isolated, treated as described below, and examined by XAS, EPR, and UV-vis spectroscopies. This subunit contains the active site for acetyl-coenzyme A synthesis, the *A-cluster*, a Ni ion bridged to an Fe₄S₄ cube. Populations of α subunits contain two major forms of A-clusters, a catalytically active form called *Ni-labile* and an inactive form called *nonlabile*. The objective of this study was to elucidate the redox and spectroscopic properties of these A-cluster forms and thereby understand their structural and functional differences. The Ni-labile form could be reduced either by CO and a catalytic amount of native enzyme or by electrochemically reduced triquat in the presence of CO. The Ni²⁺ component of the Ni-labile form reduced to Ni¹⁺ and bound CO. CO-binding raised E° for the Ni²⁺/Ni¹⁺ couple, thereby rendering CO and triquat effective reductants. Dithionite did not reduce the Ni-labile form, though its addition to CO/CODH-reduced Ni-labile clusters caused an intracuster electron transfer from the Ni¹⁺ to the [Fe₄S₄]²⁺ cluster. Dithionite reduced the [Fe₄S₄]²⁺ component of the nonlabile form, as well as the cluster of the Ni-labile form once Ni was removed. Ni may not be bridged to the cube in the nonlabile form. XAS reveals that the Ni in the nonlabile form has a distorted square-planar geometry with two N/O scatters at 1.87 Å and two S scatters at 2.20 Å. The [Fe₄S₄]²⁺ portion of Ni-labile A-clusters may maintain the Ni in a geometry conducive to reduction, CO and methyl group binding, and the migratory-insertion step used in catalysis. It may also transfer electrons to and from the redox-active D site during reductive activation.

Introduction

Carbon monoxide dehydrogenases are found in anaerobic organisms including methanogenic archaea and homoacetogenic bacteria.^{1,2} These oxygen-sensitive Ni-containing enzymes catalyze the reversible oxidation of CO to CO₂, and some of them, such as that from the homoacetogen *Clostridium thermoaceticum* (CODH),³ additionally catalyze the synthesis of acetyl-CoA from CO, coenzyme A, and a methyl group.^{4,5} This catalytic ability renders CODH a central player in the Wood–Ljungdahl pathway, which allows homoacetogens to grow autotrophically on CO₂ and H₂.^{2,6}

CODH is an $\alpha_2\beta_2$ tetramer containing three clusters called A, B, and C.⁷ The C-cluster, located in β , has a Ni-X-Fe₄S₄ structure and is the active site for the reversible oxidation of CO to CO₂.^{8–10} CO appears to bind and be oxidized at the C-cluster in an $S = 1/2$ state called C_{red1}. The resulting two-electron reduced state, C_{red2}, is thought to bind and reduce CO₂. The B-cluster, also located in β (and <15 Å from the

C-cluster),¹⁰ is an unexceptional [Fe₄S₄]^{2+/1+} cluster that functions to transfer electrons between the other clusters in the enzyme and external redox agents.^{9,11}

(3) Abbreviations: CODH, carbon monoxide dehydrogenase from *Clostridium thermoaceticum*; SDS–PAGE, sodium dodecyl sulfate polyacrylamide gel electrophoresis; DTT, dithiothreitol; phen, 1,10-phenanthroline; MV, methyl viologen; XAS, X-ray absorption spectroscopy; EPR, electron paramagnetic resonance; AP, ammonium persulfate; CoA, coenzyme A; E°_{red} , thermodynamic reduction potential at neutral pH (E°) for any of the reductants used, including oxidized/reduced triquat, bisulfite/dithionite, and CO₂/CO; E°_{dith} , E° for the bisulfite/dithionite couple; $E^\circ_{\text{Ni(labile)}}$, E° for the Ni^{2+/1+} couple in the Ni-labile form of the A-cluster; $E^\circ_{\text{Ni(nonlabile)}}$, same as $E^\circ_{\text{Ni(labile)}}$, but for the nonlabile form; $E^\circ_{\text{Ni-CO(labile)}}$, same as $E^\circ_{\text{Ni(labile)}}$, but for the effective Ni^{2+/1+}–CO couple; $E^\circ_{\text{cube(labile)}}$, E° for the [Fe₄S₄]^{2+/1+} couple in the Ni-labile form of the A-cluster; $E^\circ_{\text{cube(nonlabile)}}$, same as $E^\circ_{\text{cube(labile)}}$ but for the nonlabile form; $E^\circ_{\text{cube(depleted)}}$, same as $E^\circ_{\text{cube(labile)}}$ but for the Ni-depleted form; $E^\circ_{\text{cube(Ni-CO(labile))}}$, same as $E^\circ_{\text{cube(labile)}}$ but with CO bound at Ni¹⁺.

(4) Pezacka, E.; Wood, H. J. *Biol. Chem.* **1988**, *263*, 16000–16006.

(5) Ragsdale, S. W.; Kumar, M. *Chem. Rev.* **1996**, *96*, 2515–2539.

(6) Wood, H. G.; Ljungdahl, L. G. In *Variations in Autotrophic Life*; Shively, J. M., Barton, L. L., Eds.; Academic Press: London, 1991; pp 201–250.

(7) Xia, J.; Sinclair, J. F.; Baldwin, T. O.; Lindahl, P. A. *Biochemistry* **1996**, *35*, 1965–1971.

(8) Anderson, M. E.; DeRose, V. J.; Hoffman, B. M.; Lindahl, P. A. *J. Am. Chem. Soc.* **1993**, *115*, 12204–12205.

(9) Kumar, M.; Lu, W. P.; Liu, L. F.; Ragsdale, S. W. *J. Am. Chem. Soc.* **1993**, *115*, 11646–11647.

(10) Hu, Z. G.; Spangler, N. J.; Anderson, M. E.; Xia, J. Q.; Ludden, P. W.; Lindahl, P. A.; Münck, E. *J. Am. Chem. Soc.* **1996**, *118*, 830–845.

(11) Anderson, M. E.; Lindahl, P. A. *Biochemistry* **1994**, *33*, 8702–8711.

* To whom correspondence should be addressed. Phone: (409) 845-0956. Fax: (409) 845-4719. E-mail: Lindahl@chemvx.tamu.edu.

[†] Texas A&M University.

[‡] University of Georgia.

[§] Current address: Department of Chemistry, Swedish University of Agricultural Sciences, Box 7015, S-750 07 Uppsala, Sweden.

[⊥] Current address: Department of Microbiology, Cornell University Medical College, New York, New York 10021.

(1) *Methanogenesis*; Ferry, J. G., Ed.; Chapman & Hall: New York, 1993.

(2) *Acetogenesis*; Drake, H. L., Ed.; Chapman & Hall: New York, 1994.

The A-cluster is located in the α subunit. It also consists of an Fe_4S_4 cluster linked to a Ni through a bridge, but it serves as the active site for acetyl-CoA synthesis.^{12,13} The oxidized state of the A-cluster (A_{ox}) is diamagnetic and has the electronic distribution $\text{Ni}^{2+}\text{-X}[\text{Fe}_4\text{S}_4]^{2+}$.¹⁴ When CODH is treated with CO, A_{ox} is reduced by one electron and bound with CO to yield the $S = 1/2$ $\text{A}_{\text{red}}\text{-CO}$ state.^{15,16} $\text{A}_{\text{red}}\text{-CO}$ exhibits the NiFeC EPR signal ($g = 2.08, 2.07, 2.03$), so named because it hyperfine-broadens when enzyme is enriched in either ^{61}Ni or ^{57}Fe , or treated with ^{13}CO .¹⁷ This effect of ^{13}CO , and the results of an IR study, indicate that CO binds terminally to a metal of the reduced A-cluster.¹⁸ Münck and co-workers found that the Mössbauer isomer shift of the Fe_4S_4 component of the A-cluster was unchanged when A_{ox} reduces to the $\text{A}_{\text{red}}\text{-CO}$ state, and concluded that the added electron localizes on the Ni of $\text{A}_{\text{red}}\text{-CO}$, rather than on the Fe_4S_4 cluster (i.e., $\text{A}_{\text{red}}\text{-CO}$ corresponds to $[\text{Fe}_4\text{S}_4]^{2+}\text{-X-Ni}^{1+}\text{-CO}$).^{14,19}

Ragsdale and Wood proposed that (a) the methyl group used in the synthesis of acetyl-CoA is also bound to the Ni of the A-cluster, (b) a migratory insertion of CO into that Ni-CH₃ bond generated a Ni-acetyl, and (c) that this group was attacked by CoA to yield the product acetyl-CoA.²⁰ Subsequent results have generally been consistent with this proposal. Barondeau and Lindahl provided substantial evidence that the methyl group does bind at the Ni.²¹ Shin and Lindahl discovered that the Ni of the A-cluster can be selectively and rapidly removed using the bidentate chelate 1,10-phenanthroline (phen), and replaced by incubating phen-treated enzyme in aqueous Ni^{2+} .^{13,22} They suggested that the Ni has two cis open coordinating sites to which CO and the methyl group bind, a requirement of other migratory insertion reactions.²³

The α subunits of CODH can be isolated by adding SDS to native enzyme and subjecting the resulting mixture to electrophoresis.¹² Isolated α contains an Fe_4S_4 cluster and roughly one Ni that is coordinated, on average, to two S and two N/O ligands in a distorted square-planar geometry.²⁴ Samples of α incubated in aqueous Ni^{2+} and treated with CO and a catalytic amount of native CODH (a combination to be designated "CO/CODH") exhibit an EPR signal (called the "pseudo" NiFeC or pNiFeC signal) that mimics the ^{61}Ni , ^{57}Fe , and ^{13}CO hyperfine broadening properties of the NiFeC signal of native enzyme.²⁵ These spectroscopic similarities imply that A-clusters of isolated α and native enzyme are structurally similar.

(12) Xia, J.; Lindahl, P. A. *Biochemistry* **1995**, *34*, 6037–6042.

(13) Shin, W.; Lindahl, P. A. *Biochemistry* **1992**, *31*, 12870–12875.

(14) Xia, J.; Hu, Z.; Popescu, C. V.; Lindahl, P. A.; Münck, E. *J. Am. Chem. Soc.* **1997**, *119*, 8301–8312.

(15) Ragsdale, S. W.; Wood, H. G.; Antholine, W. E. *Proc. Natl. Acad. Sci. U.S.A.* **1985**, *82*, 6811–6814.

(16) Lindahl, P. A.; Ragsdale, S. W.; Münck, E. *J. Biol. Chem.* **1990**, *265*, 3873–3879.

(17) Fan, C.; Gorst, C. M.; Ragsdale, S. W.; Hoffman, B. M. *Biochemistry* **1991**, *30*, 431–435.

(18) Kumar, M.; Ragsdale, S. W. *J. Am. Chem. Soc.* **1992**, *114*, 8713–8715.

(19) Lindahl, P. A.; Ragsdale, S. W.; Münck, E. *J. Biol. Chem.* **1990**, *265*, 3880–3888.

(20) Ragsdale, S. W.; Wood, H. G. *J. Biol. Chem.* **1985**, *260*, 3970–3977.

(21) Barondeau, D. P.; Lindahl, P. A. *J. Am. Chem. Soc.* **1997**, *119*, 3959–3970.

(22) Shin, W.; Anderson, M. E.; Lindahl, P. A. *J. Am. Chem. Soc.* **1993**, *115*, 5522–5526.

(23) *Principles and Applications of Organotransition Metal Chemistry*; Collman, J. P., Hegedus, L. S., Norton, J. R., Finke, R. G., Eds.; University Science Books: Mill Valley, CA, 1987; Vol. Chapter 6.

(24) Xia, J.; Dong, J.; Wang, S. K.; Scott, R. A.; Lindahl, P. A. *J. Am. Chem. Soc.* **1995**, *117*, 7065–7070.

(25) Xia, J.; Lindahl, P. A. *J. Am. Chem. Soc.* **1996**, *118*, 483–484.

For unknown reasons, populations of CODH (and isolated α subunits) contain different forms of the A-cluster. Between 0 and 50% of α subunits contain a form called *Ni-labile*. This form (a) has a labile Ni, (b) can be reduced with CO/CODH to the $\text{A}_{\text{red}}\text{-CO}$ state, (c) cannot be reduced by dithionite or other low-potential reductants, (d) can bind CO and a methyl group, and (e) is catalytically active (in native enzyme). The *Ni-depleted* form is obtained when labile Ni is removed from Ni-labile A-clusters. This form is catalytically inactive and unable to achieve the $\text{A}_{\text{red}}\text{-CO}$ state, but it can be incubated with aqueous Ni^{2+} and converted back into the Ni-labile form.

About 50% of α subunits contain *nonlabile* A-clusters.¹⁴ This form (a) has a Ni that cannot be removed by phen, (b) cannot be reduced by CO (or by CO/CODH in the case of isolated α subunits), (c) can be reduced by dithionite to an $[\text{Fe}_4\text{S}_4]^{1+}$ $S = 3/2$ state, (d) cannot bind methyl groups, and (e) is not catalytically active (even in native enzyme).

Depending on the history of the sample, between 0 and 50% of α subunits contain *damaged* A-clusters. This catalytically inactive form seems to be produced at the expense of Ni-labile A-clusters when samples are treated deleteriously. Damaged A-clusters cannot be converted to the Ni-labile form by incubation in aqueous Ni^{2+} . The damaged form may or may not contain Ni, and there may actually be more than one damaged form. A number of "methods"²⁶ have been used to generate this form, including exposure to O₂ or ammonium persulfate/TEMED, or incubation in a diluted state for a prolonged period in the absence of DTT.^{14,25,27,28}

This heterogeneity was realized only after we published our earlier XAS study of isolated α ,²⁴ and it complicates those conclusions. Since the samples examined by XAS lacked the pNiFeC signal and were obtained using TEMED, ammonium persulfate, and prolonged dilution, we now suspect that about half of the A-clusters in those samples were nonlabile and half were damaged. Thus, the Ni geometry described above probably reflects the weighted average of the Ni sites in these two forms. Unfortunately, the ligand environment of the Ni in any particular A-cluster form remains undetermined.

The heterogeneity of the A-cluster is certainly a nuisance complicating the study of this already complicated metalloenzyme, but it may also be useful in identifying those structural features that render the Ni-labile form catalytically active and the nonlabile form inactive. In this paper, we present UV-vis, EPR, and XAS data of different forms of the A-cluster, and use them to characterize the different redox and structural properties of these forms. Finally, we discuss possible roles of the Fe_4S_4 moiety of the A-cluster in catalysis.

(26) We have not studied this form systematically, and these "methods" are merely post-hoc explanations of why samples were inadvertently damaged.

(27) Shin, W.; Lindahl, P. A. *Biochim. Biophys. Acta* **1993**, *1161*, 317–322.

(28) The proportion of the different A-cluster forms can be estimated from the NiFeC or pNiFeC signal intensities and the results of Xia et al. (ref 14). CODH samples exhibit NiFeC spin intensities ranging from 0 to ~ 0.4 spin/ $\alpha\beta$, with an average of roughly 0.25 spin/ $\alpha\beta$. The two ^{57}Fe -enriched samples of activated α that have been examined by Mössbauer had an average of 35% of A-clusters in the Ni-labile form, and exhibited an average pNiFeC intensity of 0.22 spin/ α . In principle, these two numbers (35% and 22%) should be equal. The reason for this discrepancy is not clear, but a similar ratio (22/35 = 0.63) was observed for a native enzyme sample, and thus it seems to be reproducible. The fraction of Ni-labile clusters in a sample is assumed to equal the (pNiFeC spin intensity)/0.63. Since the damaged form seems to arise at the expense of Ni-labile A-clusters, and these two forms together account for $\sim 50\%$ of the A-clusters in a given sample, the fraction of damaged A-clusters in a sample is $\sim 0.5 - [(\text{pNiFeC spin intensity})/(0.63)]$. The fraction of nonlabile A-clusters is presumed to be 0.5 in all samples.

Experimental Procedures

Triquat (1,1'-trimethylene-2,2'-bipyridyl) was synthesized as described²⁹ and electrochemically reduced (Princeton Applied Research potentiostat, model 273) by poisoning a stirred 22 mM solution in 50 mM Tris-Cl and 100 mM NaCl (pH 8) at -800 mV (vs Ag/AgCl) for 6 h using an Au working electrode. All subsequent potentials are given relative to NHE (normal hydrogen electrode). Protein concentrations and EPR spin quantifications were determined as described.^{30,31} UV-vis spectra were collected on a Perkin-Elmer λ 3B spectrometer using a 0.5 cm path length double-septum-sealed quartz cuvette. EPR spectra were collected on a Bruker ESP300 spectrometer with an Oxford Instruments ER910A cryostat. *Clostridium thermoaceticum* cells were grown as described.³²

Unless otherwise mentioned, all experiments involving the enzyme were performed in a Vacuum/Atmospheres Ar-atmosphere model HE-453 glovebox, containing less than 1 ppm of O₂ as monitored continuously with a calibrated Teledyne model 310 analyzer. Four preparations of CODH were purified as described.^{21,27} All were >90% pure, estimated by visually inspecting SDS-PAGE gels. Preparations 1-4 had CO oxidation activities of 300, 285, 265, and 273 units/mg and CO/acetyl-CoA exchange activities of 0.18, 0.16, 0.11, and 0.36 units/mg, respectively.^{20,33} Exchange activities were also determined in the presence of either dithionite (Aldrich) or electrochemically reduced triquat (~1 mM, final concentrations).

The α subunit was isolated as described,¹⁴ except that the gel and prerunning buffers were Tris-Cl pH 8.8 rather than boric acid, and the buffer used in both reservoirs was 0.025 M Trizma base, 0.192 M glycine, and 5 mM dithiothreitol (DTT). Typical runs used 25 mg of CODH incubated in 0.5 mL of 0.345 M SDS for 1-2 h at room temperature. Preparations of α were at least 70% pure, according to SDS-PAGE.

XAS samples were prepared as follows. Isolated α (prep 2) was freed of dithionite using a Sephadex G25 (Pharmacia) column equilibrated in 50 mM Tris pH 8, then incubated in phen (1 mM final) for 4 h, freed of phen (using Sephadex G25, as above), concentrated using a Centricon-50 (Amicon), and loaded into a 2 × 4 × 24 mm Lucite XAS cuvette with one open 4 × 24 mm face sealed with 0.025 mm Mylar tape. The cuvette was frozen on a liquid-N₂-cooled Al block, quickly removed from the glovebox, and stored in liquid N₂. XAS spectra were collected on beamline 7-3 at the Stanford Synchrotron Radiation Laboratory using a Si[220] monochromator crystal and a 13-element array of Ge detectors to measure the K α fluorescence. The storage ring contained 50-80 mA at 3.0 GeV. The sample was kept at 10 K, and 28 scans were averaged. Simultaneous energy calibration was performed by measuring the absorption of Ni foil. The EXAFSPAK³⁴ computer program package was used for EXAFS curve fitting, and feff^{35,36} version 5.04 was used to generate ab initio theoretical phase and amplitude functions.

For one UV-vis experiment, a solution of α (prep 1) was chromatographically freed of dithionite as above (except using 100 mM Tris-Cl) and mixed with NiCl₂ (1 mM, final concentration) and a catalytic amount of CODH. The resulting 400 μ L solution was incubated for 4 h, transferred into the UV-vis cuvette, and removed from the box. Sufficient thionin solution (3,7-diamino-5-phenothiazinium acetate, Aldrich) was added, using a 50 μ L Hamilton model 1705 syringe, to maximize absorbance at 420 nm (A_{420}). The cuvette was returned to the box, and 100 μ L of its contents was transferred to an

EPR tube (2.5 o.d. × 60 mm) for analysis. Another UV-vis spectrum was recorded to demonstrate that the transfer had not affected the redox state of the sample. The Ar atmosphere of the UV-vis cuvette was replaced with CO, the sample was gently agitated, and a spectrum was collected. Another aliquot was removed for EPR analysis, using a tube filled with CO. Dithionite (1 mM, final) was injected into the UV-vis cuvette, the sample was gently agitated, and spectra were collected every 5 min for 1 h. Another aliquot was removed for EPR analysis, and the remainder was used to determine protein concentration (it was 85 μ M α). In a second experiment, another sample of α was treated the same way except that dithionite (4 mM final), rather than CO, was added to thionin-oxidized α (prep 1).

In a third UV-vis experiment, a sample of α (prep 4) was separated into two aliquots. One was incubated with phen (2.5 mM final), the other with NiCl₂ (1 mM final). After 10 h, the phen-treated aliquot was freed of excess phen (by Centricon-50 dialysis), transferred to the quartz cuvette, and removed from the box. Sufficient thionin was added to maximize A_{420} , and a spectrum was recorded. Dithionite was added until A_{420} was minimized, and another spectrum was recorded. The cuvette was returned to the box, and the contents were removed for EPR and protein analyses (it was 45 μ M α). The Ni-activated α aliquot was treated equivalently.

In another experiment, a sample of isolated α (prep 3, 40 μ M) was divided into three aliquots, and each was transferred to an EPR tube (2.5 × 60 mm). One aliquot was treated with CO for 5 min and then frozen. Another was incubated with a trace of CODH and then exposed to CO as above. The third was incubated in electrochemically reduced triquat (1 mM, final concentration) and then exposed to CO as above.

Samples for the phen-inhibition study were prepared as follows. A solution of CODH (37 μ M $\alpha\beta$) was freed of dithionite as above, and divided into six ~350 μ L aliquots which were transferred into EPR tubes. One aliquot was treated with electrochemically reduced methyl viologen (Aldrich), another with Ti(III) citrate (prepared as described),³⁷ another with DTT (all reductants 1 mM, final concentration), and a fourth with 1 atm of CO. After 30 min of incubation, 10 equiv/ $\alpha\beta$ of phen was added to each tube except for one of the two that contained only CODH. All six aliquots were diluted to 400 μ L using 50 mM Tris-Cl, pH 8.0, incubated for ~12 h, exposed to CO, and then frozen for EPR analysis. An equivalent experiment was performed using thionin and oxidized methyl viologen (each 1 mM final) in place of the reductants, except that these samples reacted with phen for 2 h. A third experiment was performed using dithionite as an inhibitor. Dithionite (1.86 mM, final concentration) was added to a solution of CODH (34 μ M). An aliquot was exposed to CO, and frozen in an EPR tube. Phen (66 μ M, final concentration) was added to the remaining solution. After 20 min, a 200 μ L aliquot was transferred to an EPR tube, diluted with 200 μ L of buffer, exposed to 1 atm of CO, and frozen for analysis. Another aliquot was treated similarly after 3.5 h.

Results

Solutions of isolated α subunits contain mixtures of different forms of the A-cluster, depending on how such subunits have been treated. *Activated* α subunits (isolated subunits incubated in NiCl₂) contain a mixture of nonlabile and Ni-labile A-clusters. *Phen-treated* α subunits (isolated subunits treated with 1,10-phenanthroline) contain a mixture of nonlabile and Ni-depleted A-clusters. *As-isolated* α subunits contain a mixture of nonlabile, Ni-depleted, and Ni-labile A-clusters. *Damaged* α subunits (isolated subunits treated deleteriously) contain a mixture of nonlabile and damaged A-clusters.

XAS of 1,10-Phenanthroline-Treated Isolated α Subunit. We would like to determine the ligand environments of the Ni components of the Ni-labile and nonlabile forms of the A-cluster. This information may reveal why the former is catalytically active and the latter is not. In the absence of protein crystals, XAS studies of samples containing either Ni-labile or nonlabile A-clusters provide the best approach. At present, we

(29) Steckham, E.; Kuwana, T. *Ber. Bunsen-Ges.* **1974**, 78.

(30) Orme-Johnson, N. R.; Orme-Johnson, W. H. *Methods Enzymol.* **1978**, 52, 252-257.

(31) Pelley, J. W.; Garner, C. W.; Little, G. H. *Anal. Biochem.* **1978**, 86, 341-343.

(32) Lundie, L. L., Jr.; Drake, H. L. *J. Bacteriol.* **1984**, 159, 700-703.

(33) Ramer, S. E.; Raybuck, S. A.; Orme-Johnson, W. H.; Walsh, C. T. *Biochemistry* **1989**, 28, 4675-4680.

(34) The EXAFSPAK program was developed by Graham N. George and is available on the SSRL Web site at <http://ssrl01.slac.stanford.edu/exafspak.html>.

(35) Rehr, J. J.; Mustre de Leon, J.; Zabinsky, S. I.; Albers, R. C. *J. Am. Chem. Soc.* **1991**, 113, 5135-5140.

(36) Mustre de Leon, J.; Rehr, J. J.; Zabinsky, S. I.; Albers, R. C. *Phys. Rev.* **1991**, B44, 4146-4156.

(37) Zehnder, A. J. B.; Wuhmann, K. *Science* **1976**, 194, 1165-1166.

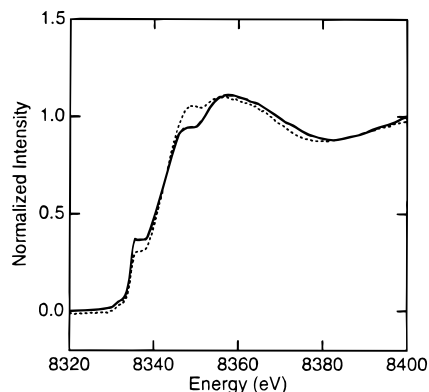


Figure 1. Ni X-ray absorption edge spectra of phen-treated (dotted line) and as-isolated α subunit (solid line).²⁴

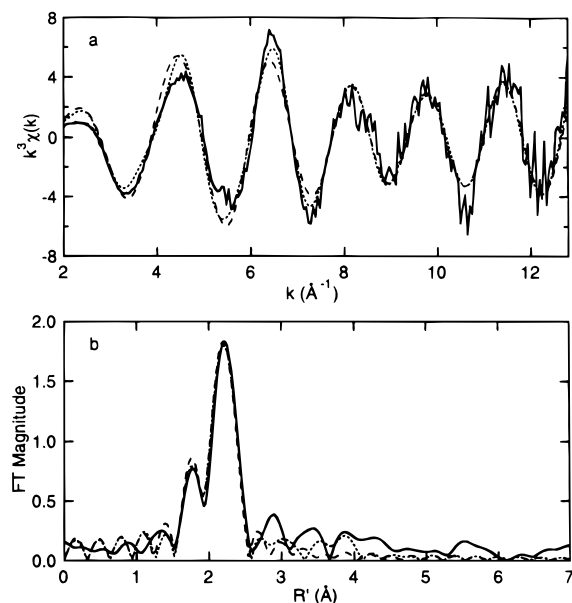


Figure 2. k^3 -weighted EXAFS (a) and Fourier transform (b) (over the range $k = 2\text{--}12 \text{ \AA}^{-1}$) of phen-treated α subunit (solid line) including NiS_2N_2 fits, with (dotted line) and without (dashed line) imidazole ligands.

have no means of preparing samples of pure Ni-labile A-clusters, but phen treatment does result in samples of α for which all of the Ni arises from nonlabile A-clusters. Such a sample was examined by XAS, and the resulting Ni-edge and EXAFS spectra are shown in Figures 1 and 2. The edge included a feature at 8338 eV arising from a $1s \rightarrow 4p_z$ plus shakedown transition. This feature is present in square-planar complexes and is absent in tetrahedral ones, and its relative intensity can be used to assess the dihedral angle distorting a complex from pure square-planar symmetry. When compared with model compounds, the intensity of such a feature in spectra of our previous sample of isolated α subunits suggested that the average Ni environment had a distorted square-planar geometry with a $20\text{--}30^\circ$ dihedral-angle twist.²⁴ The slightly lower intensity of the feature in the edge spectrum of the current phen-treated sample indicates a slightly larger dihedral angle for the Ni geometry of the nonlabile form.

Ni EXAFS data, the Fourier transform (FT), and curve-fitting results are shown in Figure 2, and the best-fit parameters are given in Table 1. The data fit best to two N/O scatterers at 1.87 \AA and two S scatterers at 2.20 \AA . The FT features between 2 and 4 \AA may result from multiple scattering from histidines, since the multiple scattering fit with two imidazoles is somewhat better than the single scattering $\text{Ni}(\text{N/O})_2\text{S}_2$ fit.

Table 1. EXAFS Curve Fitting Results for Phen-Treated α Subunits^a

fit	shell	N_s	R_{as} (\AA)	σ_{as}^2 (\AA^2)	ΔE_o (eV)	f'
single scattering	Ni-S	(2)	2.20	0.0018	-6.21	0.087
	Ni-N	(2)	1.87	0.0039	[-6.21]	(0.066)
multiple scattering	Ni-S	(2)	2.19	0.0019	-4.41	0.079
	Ni-N	(2)	1.87	0.0039	[-4.41]	(0.057)
	Ni-N	(2)	[3.96]	[0.0083]	[-4.41]	
	Ni-C	(2)	[2.82]	[0.0062]	[-4.41]	
	Ni-C	(2)	[2.93]	[0.0062]	[-4.41]	
	Ni-C	(2)	[4.03]	[0.0085]	[-4.41]	

^a N_s is the number of scatterers (or groups) per metal. R_{as} is the metal-scatterer distance. σ_{as}^2 is a mean square deviation in R_{as} . ΔE_o is the shift in E_o for the theoretical scattering functions. f' is a normalized error (χ^2): $f' = \{\sum_i [k^3(\chi_i^{obs} - \chi_i^{calc})^2/N]^{1/2} / [(k^3\chi^{obs})_{max} - (k^3\chi^{obs})_{min}]\}$. Numbers in angle brackets are f' for smoothed data. Numbers in parentheses were not varied during optimizations. Numbers in square brackets were constrained to be a multiple of the above value (σ_{as}^2) or to maintain a constant difference (R_{as} , ΔE_o).

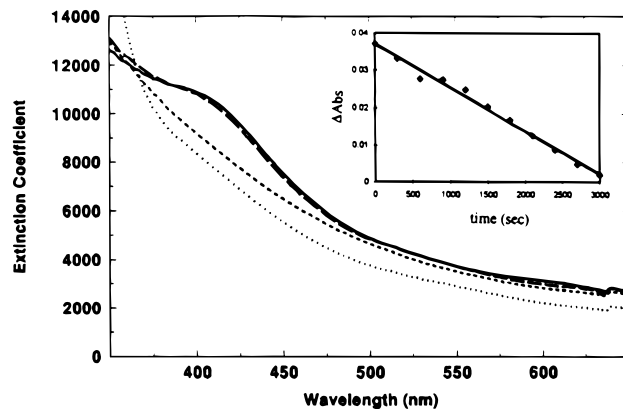


Figure 3. Electronic absorption spectrum of activated α subunit. Solid line, oxidized; long-dashed line, reduced with CO/CODH; short-dashed line, reduced with dithionite; dotted line, reduced with CO/CODH and dithionite. Inset: Intensity at 420 nm vs time. The solid line is the least-squares best fit to the data.

UV-Vis and EPR of Activated α Subunits Reduced with CO/CODH.

Xia et al. recently concluded, from a Mössbauer/EPR study of the activated α subunit (containing a mixture of Ni-labile and nonlabile forms), that the Fe_4S_4 component of $\text{A}_{red}\text{-CO}$ is in the $2+$ core oxidation state, and that the Ni is in the $1+$ oxidation state with CO bound.¹⁴ We tested their conclusion by examining the electronic absorption and EPR spectra of activated α in the oxidized and CO/CODH-reduced states. Oxidized α exhibited a strong shoulder at $\sim 420 \text{ nm}$ (Figure 3, solid line) and no EPR signals (Figure 4, solid lines). The absorption feature was due to $S \rightarrow \text{Fe}$ charge-transfer transitions arising from the $S = 0$ $[\text{Fe}_4\text{S}_4]^{2+}$ component of both the Ni-labile and nonlabile forms of the A-cluster. (Spectral features due to the Ni^{2+} component of the A-cluster have not been identified and are presumably obscured by the $S \rightarrow \text{Fe}$ absorption.) When these clusters are reduced to the $1+$ state, the intensity at 420 nm declines. However, treating the oxidized sample with CO/CODH had little effect on the absorption shoulder at 420 nm (Figure 3, long-dashed line). Relative to the spectrum of what appears to be fully reduced α (see below), the extent of decline indicates that only $\sim 1\%$ of the Fe_4S_4 clusters in the sample were reduced by this treatment. CO/CODH cannot reduce nonlabile A-clusters (they remain A_{ox} , with the Fe_4S_4 cluster in the $2+$ state), but this combination can reduce the Ni-labile form to the $\text{A}_{red}\text{-CO}$ state. That this reduction actually occurred in the sample examined was evidenced by the presence of the pNiFeC signal (Figure 4A,

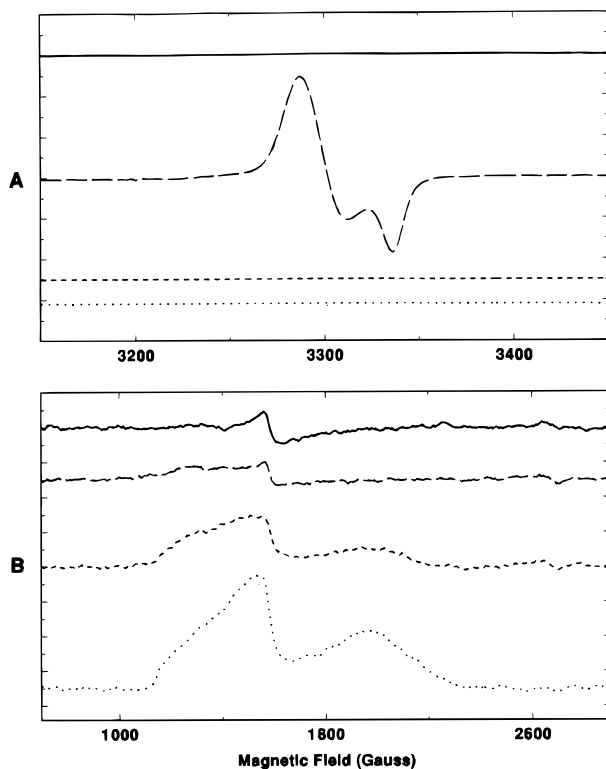


Figure 4. High-field (A) and low-field (B) EPR spectra of the activated α subunit. Solid line, oxidized; long-dashed line, reduced with CO/CODH; short-dashed line, reduced with dithionite; dotted line, reduced with CO/CODH and dithionite. EPR conditions: microwave frequency, 9.43 GHz; microwave power, 80 (A) and 20 (B) mW; temperature, 130 (A) and 10 (B) K. Spectra have been offset for clarity.

long-dashed line) with an intensity of 0.18 spins/ α . Such a spin intensity indicates that about 28% of the clusters in the sample were in the $A_{\text{red-CO}}$ state.^{14,28}

The lack of spectral decline at 420 nm proportionate to the fraction of Ni-labile A-clusters reduced in this sample (28% in this case) indicates that the Fe_4S_4 component of $A_{\text{red-CO}}$ is in the 2+ core oxidation state. The absence of EPR features between $g = 4-6$ (Figure 4B, long-dashed line) confirms that nonlabile A-clusters are not reduced by CO/CODH to the $S = 3/2$ $[\text{Fe}_4\text{S}_4]^{1+}$ state.

UV-Vis and EPR of Activated α Subunits Reduced with Dithionite and CO/CODH/Dithionite. Another sample of oxidized activated α was reduced with dithionite and examined by UV-vis and EPR spectroscopies (Figures 3 and 4, short-dashed lines). Relative to the spectrum of what appears to be fully reduced α (Figure 3, dotted line, see below), the extent of decline ($67 \pm 3\%$, average of four trials) and the development of features at $g = 4-6$ (Figure 4B, short-dashed line) indicates that $\sim 67\%$ of the Fe_4S_4 clusters in the sample were reduced to the $S = 3/2$ $[\text{Fe}_4\text{S}_4]^{1+}$ state by dithionite. Xia et al. reported that dithionite can reduce nonlabile A-clusters to the $S = 3/2$ state, and presented some Mössbauer evidence that dithionite cannot reduce the Ni-labile form.¹⁴ Our UV-vis and EPR results provide further support for these conclusions.

The electronic absorption spectrum of the CO/CODH/dithionite-reduced sample, collected immediately after adding dithionite to the CO/CODH-reduced sample, was $\sim 65\%$ reduced, similar to that exhibited by the sample treated only with dithionite. However, during the next 90 min, the absorption shoulder declined in intensity, eventually yielding the spectrum of Figure 3, dotted line. A plot of the log of the intensity at 420 nm vs time (Figure 3, inset) indicates an apparent zero-

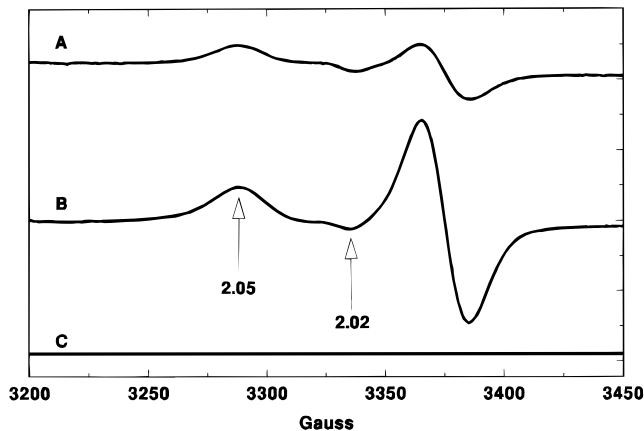


Figure 5. High-field EPR spectra of activated α subunits reduced with triquat in the presence of CO. (A) Activated α plus CO/CODH. (B) Activated α plus CO/triquat. (C) Activated α plus CO. EPR conditions as in Figure 4A. Numbers under the arrows indicate g values. We have been unable to identify the small radical feature at $g = 2.0$ in spectrum A. The larger radical feature in spectrum B is primarily due to reduced triquat.

order decay constant of $1.1 \times 10^{-5} \text{ M s}^{-1}$. The absence of a shoulder in the 420 nm region is typical of fully reduced $[\text{Fe}_4\text{S}_4]^{1+}$ clusters, and it (along with our inability to reduce the sample further) suggests that all the clusters in α are reduced by the CO/CODH/dithionite combination. This conclusion is supported by EPR spectra of the CO/CODH/dithionite-reduced sample (Figure 4 dotted lines), which were devoid of the pNiFeC signal but exhibited low-field features typical of $S = 3/2$ $[\text{Fe}_4\text{S}_4]^{1+}$ clusters, at an intensity roughly twice that of the dithionite-reduced sample. Moreover, $\Delta\epsilon_{420}$ ($3600 \text{ M}^{-1} \text{ cm}^{-1}$ for four trials, averaged), the difference between the extinction coefficients of the oxidized and CO/CODH/dithionite-reduced sample, was similar to that obtained for unactivated α ($4000 \text{ M}^{-1} \text{ cm}^{-1}$).²⁴ A dithionite-reduced unactivated sample has been shown by Mössbauer to be fully reduced.¹⁴ Discrepancies in $\Delta\epsilon_{420}$ between the two samples are likely caused by minor errors in protein concentration determinations.

Taken together, these results indicate that (a) in the absence of CO/CODH, dithionite reduces nonlabile A-clusters (to the $S = 3/2$ $[\text{Fe}_4\text{S}_4]^{1+}$ state) but not Ni-labile clusters, (b) in the absence of dithionite, CO/CODH reduces Ni-labile A-clusters (to the $A_{\text{red-CO}}$ state), but not nonlabile clusters, (c) in the presence of both CO/CODH and dithionite, both Ni-labile and nonlabile A-clusters are reduced (to the $S = 3/2$ state), and (d) in the presence of CO/CODH/dithionite, nonlabile A-clusters reduce substantially faster (within the time of manual mixing) than the Ni-labile ones.

EPR of Activated α Subunits Reduced with Triquat in the Presence of CO. Shin and Lindahl noted that although CO and dithionite have comparable redox potentials ($E^\circ \approx -0.55 \text{ V}$), only CO can reduce Ni-labile A-clusters.¹³ They suggested that the binding of CO to the A-cluster raised the $A_{\text{ox}}/A_{\text{red}}$ redox potential, thereby rendering reductants with $E^\circ \approx -0.55 \text{ V}$ effective. The inability of dithionite, in the presence of CO, to reduce the Ni-labile form of α to the $A_{\text{red-CO}}$ state appears to be evidence *against* this proposal. However, we suspected that dithionite is not an innocent reductant, and decided to repeat the experiment using electrochemically reduced triquat, a low-potential ($E^\circ = -540 \text{ mV}$), noncoordinating reductant. A sample of α was split into three aliquots. One was reacted with CO, another with CO/CODH, and the third with CO and triquat (CO/triquat). The CO/CODH and CO/triquat samples exhibited the pNiFeC signal (Figure 5A,

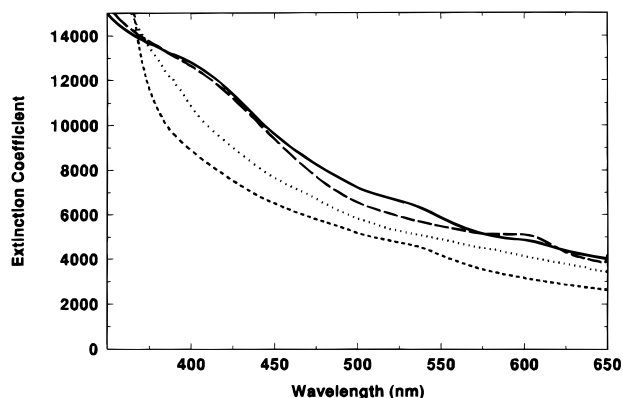


Figure 6. Electronic absorption spectrum of phen-treated and activated α subunit. Solid line, oxidized phen-treated; long-dashed lines, oxidized activated α subunits; dotted line, dithionite-reduced phen-treated; short-dashed line, dithionite-reduced activated α subunits.

0.05 spin/ α , and Figure 5B, 0.11 spin/ α , respectively), while the sample reacted with CO alone afforded no signal (Figure 5C). This indicates that in the presence of CO, triquat reduced the Ni-labile form of the A-cluster to the $A_{\text{red}}\text{-CO}$ state, it provides evidence that the binding of CO does increase the $A_{\text{ox}}/A_{\text{red}}$ redox potential, and it supports our suspicion that dithionite is a noninnocent reductant that may interact with the A-cluster.

A further study was performed to assess the effect of dithionite on the A-cluster. Dithionite has been reported to inhibit the CO/acetyl-CoA exchange activity of CODH,²⁰ and our studies confirm this (1 mM dithionite completely inhibited this activity). In contrast, the activity was only inhibited 15% by 1 mM triquat (data not shown). Since both reductants have similar redox potentials, these results suggest that dithionite inhibits the chemistry occurring at Ni-labile A-clusters, not by reducing the enzyme, but by binding to a site on CODH.

Electronic Absorption Spectra of Phen-Treated and Activated α Subunits Reduced with Dithionite. To determine whether dithionite could reduce Ni-depleted A-clusters, a sample of as-isolated α was divided in two; half was treated with phen and half with NiCl_2 . The phen-treated and Ni-activated samples were oxidized with a trace of thionin, and examined by electronic absorption spectroscopy (Figure 6, solid and long-dashed lines, respectively). Then dithionite was added to each, and spectra were again obtained (Figure 6, dotted and short-dashed lines, respectively). Dithionite reduced the phen-treated sample fully, affording $\Delta\epsilon_{420} = 3900 \text{ M}^{-1} \text{ cm}^{-1}$. This indicates that dithionite can reduce Ni-depleted A-clusters to the $[\text{Fe}_4\text{S}_4]^{1+}$ state.³⁹ The partial reduction of the Ni-activated sample by dithionite ($\Delta\epsilon_{420} = 2100 \text{ M}^{-1} \text{ cm}^{-1}$) provides further evidence that dithionite reduces nonlabile A-clusters but not Ni-labile ones. These conclusions are supported by corresponding EPR spectra (Figure 7). The spectrum of the dithionite-reduced phen-treated sample (A) exhibited features in the $g = 4\text{--}6$ region, which are typical of $S = 3/2$ $[\text{Fe}_4\text{S}_4]^{1+}$ clusters, with an intensity noticeably greater than those of the dithionite-reduced Ni-activated sample (B).

Effect of Reductants on Phen's Ability To Remove Labile Ni. To determine whether the redox state of the enzyme affects phen's ability to remove the labile Ni of the A-cluster, a series of CODH samples were treated with several reductants and

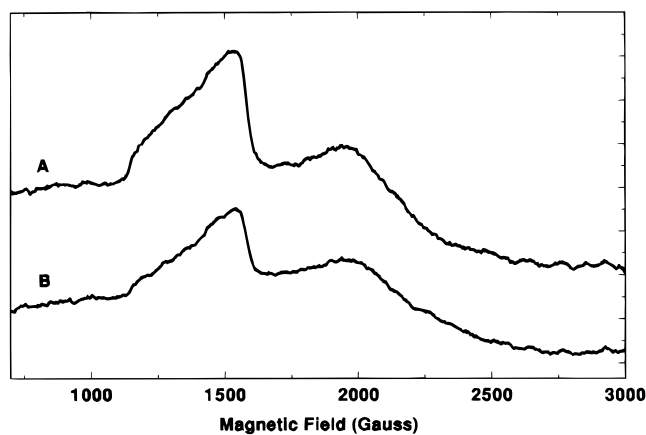


Figure 7. Low-field EPR of phen-treated (A) and Ni-activated (B) α subunits reduced with dithionite. EPR conditions as in Figure 4B.

Table 2. Inhibition of Phen by Redox Mediators

inhibitor	phen incubation time (h)	% labile-Ni remaining ^a ($\pm 10\%$)
Ti(III) citrate	12	98
CO	12	103
MV ⁺	12	65 ⁴⁰
DTT	12	70
dithionite	3.5	109
thionin	2	10
MV ²⁺	2	7
(none)	2	4

^a The percentage of labile-Ni remaining is determined by dividing the quantified NiFeC signal intensity of the sample of interest with that of a sample that was not exposed to phen, and then multiplying by 100.

oxidants, including CO, dithionite, Ti(III) citrate, DTT, reduced and oxidized methyl viologen, and thionin. As summarized in Table 2, the reductants inhibited phen's ability to remove labile Ni, while the oxidants had no effect.⁴⁰ The nature of the reductant seemed irrelevant with regard to its effectiveness. These results suggest that the reduction of some site on the enzyme, rather than the binding of the reductant to the enzyme, inhibited phen from removing the labile Ni. Effective inhibitors had redox potentials between -0.44 and -0.58 V, suggesting that the site reduced had a similar or greater $E^{\circ'}$. The only exception was DTT, which effectively inhibited the Ni-removal reaction, but has a redox potential of -0.33 V at pH 7.⁴¹

Discussion

Figure 8 summarizes our proposed structures and chemical properties of the Ni-labile, nonlabile, and Ni-depleted A-cluster forms. We present it at the outset of the Discussion and suggest that it be used as a reference and guide for this section.

Since the conversion of A_{ox} to $A_{\text{red}}\text{-CO}$ was not associated with a spectral decline at 420 nm, the electron used in that reduction does not appear to localize on the Fe_4S_4 component of the A-cluster. This supports and establishes the conclusion of Lindahl et al. and Xia et al. that this electron localizes on the Ni.^{19,14,42} Thus, reduction of A_{ox} to $A_{\text{red}}\text{-CO}$ corresponds

(40) The blue color of the methyl viologen/phen/CODH solution disappeared during the experiment, and it returned upon treatment with CO. Thus, reduced methyl viologen did not completely inhibit the removal of Ni, apparently because the solution became oxidized during the course of the reaction.

(41) *The Merck Index*, 11th ed.; Budavari, S., Ed.; Merck & Co., Inc.: Rahway, NJ, 1989; p 533.

(42) For further discussion relevant to this assignment see: Qiu et al. *J. Am. Chem. Soc.* **1997**, *119*, 11134. Spiro, T. G. *Science* **1997**, *278*, 21.

(38) Reference deleted on revision.

(39) We have some circumstantial evidence suggesting that prolonged reaction of α with high concentrations of phen damages Ni-labile A-clusters. Thus, the samples prepared here are certainly "Ni-depleted" in that they are devoid of labile Ni, but they may not reactivate fully if incubated with NiCl_2 .

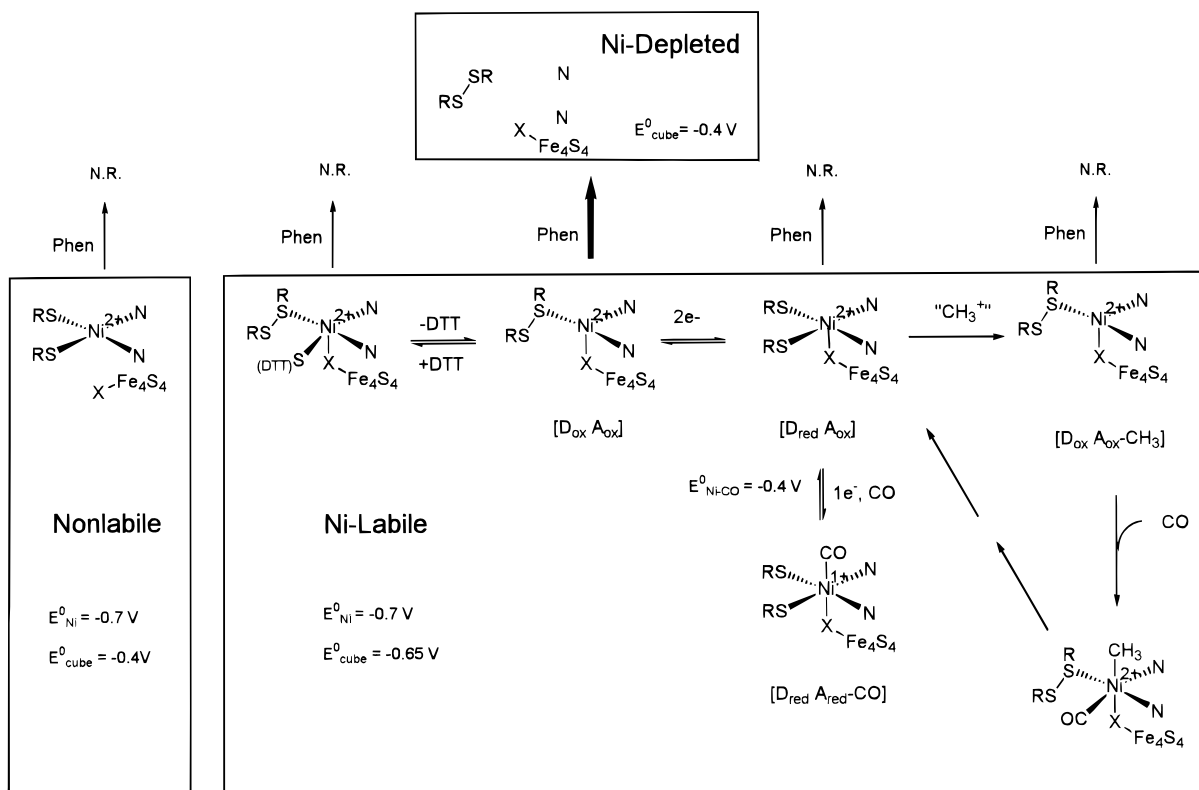


Figure 8. Proposed structures and the redox couples of the cube and Ni present in the Ni-labile, nonlabile, and Ni-depleted forms. All structures within the large box represent the Ni-labile form in different states. Novel proposed steps in the catalytic cycle (right side of large box) are indicated. Other steps (migratory insertion and nucleophilic attack by CoA on the Ni-acetyl) are the same as proposed previously.²¹

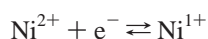
to the effective redox couple



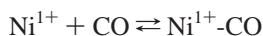
or more simply



with effective redox potential $E^{\circ'}_{\text{Ni-CO(labile)}}$. This effective redox couple is composed of a true $\text{Ni}^{2+}/\text{Ni}^{1+}$ redox couple with $E^{\circ'}_{\text{Ni(labile)}}$



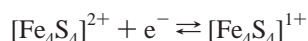
and a CO-binding reaction



with binding constant K_{CO} . The effective redox potential $E^{\circ'}_{\text{Ni-CO(labile)}}$ is obtained from $E^{\circ'}_{\text{Ni(labile)}}$ and K_{CO} according to the relationship⁴³

$$E^{\circ'}_{\text{Ni-CO(labile)}} = E^{\circ'}_{\text{Ni(labile)}} + 0.059 \log K_{\text{CO}}$$

In the E° nomenclature to be used, the form of the A-cluster to which the redox couple refers will be subscripted and placed in parentheses, and this will be preceded by the component of the A-cluster that is being reduced. Thus, E° corresponding to reduction of the Fe_4S_4 cube in the nonlabile form,



will be designated $E^{\circ'}_{\text{cube(nonlabile)}}$.

Our results, combined with those of earlier studies,^{14,19} show that CO/CODH and CO/triquat reduce the Ni-labile form of the A-cluster to the $S = 1/2$ $A_{\text{red-CO}}$ state, that CO/dithionite reduces this form to the $S = 3/2$ $[\text{Fe}_4\text{S}_4]^{1+}$ state, and that dithionite alone does not reduce the Ni-labile form. We explain these results with the following model: Dithionite (and other reductants with $E^{\circ'}_{\text{red}} \approx -0.55$ V) cannot reduce the Ni-labile form of the A-cluster in the absence of CO (i.e. in the A_{ox} state) because the $E^{\circ'}$ values associated with the $\text{Ni}^{2+/1+}$ and $[\text{Fe}_4\text{S}_4]^{2+/1+}$ couples ($E^{\circ'}_{\text{Ni(labile)}}$ and $E^{\circ'}_{\text{cube(labile)}}$) are substantially more negative than $E^{\circ'}_{\text{red}}$. The binding of CO to the A-cluster raises the labile $\text{Ni}^{2+/1+}$ potential such that low-potential reductants (CO/CODH and CO/triquat) reduce A_{ox} to $A_{\text{red-CO}}$ (i.e., $E^{\circ'}_{\text{Ni(labile)}} < E^{\circ'}_{\text{red}} < E^{\circ'}_{\text{Ni-CO(labile)}}$). The fact that the electron localizes on the Ni rather than the cube suggests that $E^{\circ'}_{\text{cube(Ni-CO(labile))} < E^{\circ'}_{\text{Ni-CO(labile)}}$, and it seems reasonable to presume (given that CO is almost certainly bound to Ni^{1+} in the $A_{\text{red-CO}}$ state) that the redox potential of the cube is not significantly affected by this binding (i.e., $E^{\circ'}_{\text{cube(labile)}} \approx E^{\circ'}_{\text{cube(Ni-CO(labile))}$). This model can be summarized as

$$[E^{\circ'}_{\text{Ni(labile)}} \approx E^{\circ'}_{\text{cube(labile)}} \approx E^{\circ'}_{\text{cube(Ni-CO(labile))}] < E^{\circ'}_{\text{red}} < E^{\circ'}_{\text{Ni-CO(labile)}}$$

Two studies which illustrate the effect of CO binding on redox potentials influenced formulation of our model. Darensbourg and co-workers found that the redox potential of [1,5-bis(mercapto-ethyl)-1,5-diazacyclooctane]Ni(II) increased by 100 mV in the presence of CO ($E^{\circ}_{\text{Ni}} < E^{\circ}_{\text{Ni-CO}}$).⁴⁴ Lewis and Schröder (1982) reduced a Schiff-base tetrazamacrocycle of Ni^{2+} by one electron.⁴⁵ In the absence of CO, the electron localized

(43) Russell, W. K.; Lindahl, P. A. *Biochemistry*, in press.

(44) Musie, G.; Reibensies, J. H.; Darensbourg, M. Y. *Inorg. Chem.* **1998**, *37*, 302–310.

on the ligand (yielding an isotropic EPR signal at $g = 2.002$) while with CO bound at the Ni, the electron localized on the Ni^{1+} (yielding EPR with $g_{\parallel} = 2.211$ and $g_{\perp} = 2.050$). Thus, the binding of CO appears to raise E° of the $\text{Ni}^{2+/1+}$ couple above $E^{\circ}_{\text{ligand}}$ of the $\text{ligand}_{\text{ox}}/\text{ligand}_{\text{red}}$ couple and induces an intramolecular electron transfer from the ligand to the Ni. This situation can be summarized by assuming the following order of redox potentials:

$$E^{\circ}_{\text{Ni}} < E^{\circ}_{\text{red}} < E^{\circ}_{\text{ligand}} < E^{\circ}_{\text{Ni-CO}}$$

The model describing the redox properties of the Ni-labile A-cluster predicts that treatment with CO/dithionite should also afford the $\text{A}_{\text{red}}\text{-CO}$ state (rather than the observed $S = 3/2$ $[\text{Fe}_4\text{S}_4]^{1+}$ state). The only explanation apparent to us, which would not “unravel” the model just presented, is that dithionite serves not to reduce the cube but to accelerate the dissociation of CO from the Ni (possibly by interacting with the Ni). Our results (showing that dithionite inhibited CO/acetyl-CoA exchange activity but the noncoordinating triquat did not) support this possibility. It seems likely that dithionite binds to the A_{ox} state rather than $\text{A}_{\text{red}}\text{-CO}$. If dithionite replaced CO by binding to Ni^{1+} of what had been the $\text{A}_{\text{red}}\text{-CO}$ state, it would need to bind tighter than CO bound. However, that would cause E°_{Ni} to increase to even higher potentials. In contrast, if dithionite binds to Ni^{2+} , it would cause a decrease in potential, as observed. We suggest that the dithionite-induced loss of CO lowers E°_{Ni} below E°_{cube} , and that an electron transfers from Ni^{1+} to the $[\text{Fe}_4\text{S}_4]^{2+}$ cube. Such an intracluster electron-transfer implies that $E^{\circ}_{\text{Ni}(\text{labile})} < E^{\circ}_{\text{cube}(\text{labile})}$. The apparent rate constant for this intracluster electron transfer ($1.1 \times 10^{-5} \text{ M s}^{-1}$) seems too slow for the process to be mechanistically important, but two processes (loss of CO from Ni^{1+} and the subsequent electron transfer from Ni^{1+} to the $[\text{Fe}_4\text{S}_4]^{2+}$ cube) are involved, and if loss of CO is rate-limiting, electron transfer may be far faster than the overall rate measured here. This raises the possibility that, during catalysis, electrons transfer between the cube and the Ni, and that the cube functions as an electron transfer conduit. Dithionite may not behave exactly in this manner with native CODH, since adding dithionite to CO-reduced CODH does not abolish the NiFeC signal. This implies that, in native enzyme, either CO binds more tightly or dithionite binds less tightly vis-à-vis the respective binding to isolated α .

The ability of CO/triquat to reduce A_{ox} to $\text{A}_{\text{red}}\text{-CO}$ is the first unambiguous evidence that a reductant other than CO can reduce Ni-labile A-clusters, and it indicates that CO binding raises the potential of the $\text{Ni}^{2+/1+}$ couple. This result also argues against the idea that non-CO low-potential reductants such as dithionite and triquat are kinetically barred from reducing A_{ox} (e.g., that the cluster organization in the enzyme only allows electrons obtained by the oxidation of CO at the C-cluster to reduce A_{ox}). Prior to this study the only evidence against this idea was that A_{ox} of cyanide-inhibited CODH reduced faster to $\text{A}_{\text{red}}\text{-CO}$, after exposure to CO, than CN^- dissociated from the C-cluster.¹¹ Anderson and Lindahl concluded that dithionite must have reduced the A_{ox} directly because the C-cluster is inoperative when bound with cyanide. The idea that the electron reducing A_{ox} must come from CO oxidation at the C-cluster also seems unlikely given the redox properties of the C-cluster. Both CO and dithionite reduce C_{ox} to $\text{C}_{\text{red}2}$,^{11,16,46} and once $\text{C}_{\text{red}2}$ is obtained, it would be difficult to rationalize why electrons from

$\text{C}_{\text{red}2}$ would reduce A_{ox} when CO, but not dithionite, had been the reductant.

We also found that dithionite reduces Ni-depleted A-clusters to the $S = 3/2$ $[\text{Fe}_4\text{S}_4]^{1+}$ state. Thus, loss of Ni and the cube species bridging the Ni and the cube appears to raise E°_{cube} such that dithionite can reduce it (i.e. $E^{\circ}_{\text{cube}(\text{Ni-CO}(\text{labile}))} < E^{\circ}_{\text{dith}} < E^{\circ}_{\text{cube}(\text{depleted})}$). Similarly, dithionite reduces the nonlabile form to the $S = 3/2$ $[\text{Fe}_4\text{S}_4]^{1+}$ state, suggesting that $E^{\circ}_{\text{cube}(\text{nonlabile})} \approx E^{\circ}_{\text{cube}(\text{depleted})}$. Thus, the redox properties of the cube in the Ni-labile form convert to those in the nonlabile form upon loss of the Ni and/or bridge. Since Ni is present in nonlabile A-clusters, this suggests that the factor effecting that conversion is not loss of Ni per se, but loss of the bridge. The simplest explanation is that the Ni in the nonlabile form is electronically disconnected from the cube; i.e., that there is no bridge linking the Ni and cube in the nonlabile form.

Our results show that CO/CODH cannot reduce the nonlabile form. The Ni of this form appears to be redox inactive Ni^{2+} and we have evidence that it does not bind CO.^{24,47} Hence, it is likely that $E^{\circ}_{\text{Ni}(\text{nonlabile})} \leq E^{\circ}_{\text{Ni}(\text{labile})} < E^{\circ}_{\text{CO/CODH}}$. According to the thermodynamics of our model, CO/CODH should reduce the cube of the nonlabile form to the $S = 3/2$ state. We are uncertain how “CO/CODH” reduces isolated A-clusters in α subunits, but it probably involves an electron transfer from a cluster in CODH which was itself reduced by electrons obtained from the oxidation of CO at the C-cluster. The large size of CODH (310 kDa) suggests that it may be ineffective because the cube of the A-cluster is buried. A similar argument regarding the Ni of the A-cluster would be less compelling since it can be methylated by an 89 kDa corrin-iron-sulfur protein.^{5,48} In fact, this function of the Ni suggests that it is located at or near the surface of the α subunit. Thus, the picture most consistent with our results would have the cube of the A-cluster directed toward the interior of α and bridged to a surface-exposed Ni.

In summary, our model indicates the following ordering of redox potentials:

$$\begin{aligned} E^{\circ}_{\text{Ni}(\text{nonlabile})} &\leq E^{\circ}_{\text{Ni}(\text{labile})} < E^{\circ}_{\text{cube}(\text{labile})} \approx \\ &E^{\circ}_{\text{cube}(\text{Ni-CO}(\text{labile}))} < E^{\circ}_{\text{red}} < E^{\circ}_{\text{Ni-CO}(\text{labile})} \approx \\ &E^{\circ}_{\text{cube}(\text{nonlabile})} \approx E^{\circ}_{\text{cube}(\text{depleted})} \end{aligned}$$

E° for $[\text{Fe}_4\text{S}_4]^{2+/1+}$ clusters in proteins average around -0.4 V,⁴⁹ and the behavior of the cubes in the nonlabile and Ni-depleted forms suggests similar E° values. E°_{red} for CO, dithionite and triquat, at pH 8, are -0.58 , -0.55 , and -0.54 V, respectively.^{29,50,51} We recently determined the effective redox potential $E^{\circ}_{\text{Ni-CO}(\text{labile})}$ (designated E°_{NiFeC} in ref 43) to be about -0.44 V.⁴³ $E^{\circ}_{\text{Ni}(\text{labile})}$ (designated E°_{A} in ref 43) could not be determined unequivocally, because the binding constant for CO to Ni^{1+} is not known. Using realistic constraints, we concluded that $E^{\circ}_{\text{Ni}(\text{labile})}$ is between -0.49 and -0.69 V (each factor-of-ten increase in K_{CO} shifts $E^{\circ}_{\text{Ni}(\text{labile})}$ more negatively from $E^{\circ}_{\text{Ni-CO}(\text{labile})}$ by 0.06 V). The fact that dithionite and triquat do not noticeably reduce Ni in the Ni-labile form in the absence of CO suggests that $E^{\circ}_{\text{Ni}(\text{labile})}$ is at least 0.1 V more negative than E°_{red} (i.e., less than ~ -0.65 V), and that K_{CO} is

(47) Fraser, D. M.; Lindahl, P. A. Manuscript in preparation.

(48) Halcrow, M. A.; Christou, G. *Chem. Rev.* **1994**, *94*, 2421–2481.

(49) Stephans, P. J.; Jollie, D. R.; Warshel, A. *Chem. Rev.* **1996**, *96*, 2491–2513.

(50) Butler, J. N., *Carbon Dioxide Equilibria and Their Applications*; Addison-Wesley: Reading, MA, 1982.

(51) Mayhew, S. G.; Petering, D.; Palmer, G.; Faust, G. P. *J. Biol. Chem.* **1969**, *244*, 2830–2834.

(45) Lewis, J.; Schröder, M. *J. Chem. Soc., Dalton Trans.* **1982**, 1085.

(46) Anderson, M. E.; Lindahl, P. A. *Biochemistry* **1996**, *35*, 8371–8380.

quite strong ($>10^4 \text{ atm}^{-1}$ which is comparable to the binding strength of CO to deoxymyoglobin).⁵² A similar argument can be made for $E^{\circ'}_{\text{cube(labile)}}$; it is probably less than or equal to -0.65 V , since dithionite cannot reduce the cube in the Ni-labile form. Finally, $E^{\circ'}_{\text{Ni(labile)}}$ should be less than $E^{\circ'}_{\text{cube(labile)}}$, for the intracuster electron transfer goes spontaneously from the Ni to the cube. However, $E^{\circ'}_{\text{Ni(labile)}}$ is probably not much lower than $E^{\circ'}_{\text{cube(labile)}}$, for this would require unreasonably large K_{CO} values. We suggest -0.70 V for $E^{\circ'}_{\text{Ni(labile)}}$ and -0.65 V for $E^{\circ'}_{\text{cube(labile)}}$. These proposed redox potentials are summarized in Figure 8.

To summarize our model, the bridge to the Ni in the Ni-labile form stabilizes the cube in the 2+ core oxidation state. The Ni in this form becomes reduced and binds CO, forming $\text{Ni}^{1+}\text{-CO}$. Dithionite accelerates the loss of CO from this Ni^{1+} , inducing an intracuster electron transfer from the Ni to the cube. In the nonlabile form, the Ni is effectively redox inactive and in the Ni^{2+} state, there may not be a bridge to the cube, and the cube can readily be reduced to the 1+ core oxidation state. The cube of the nonlabile form is kinetically inaccessible to large reductants such as CODH. In phen-treated α , the labile Ni and bridge are lost and this raises the redox potential of the cube, allowing it to assume the redox properties of the cube in the nonlabile form.

The XAS spectra of phen-treated α , which reflects only Ni in nonlabile A-clusters, indicate that nonlabile Ni has distorted square-planar geometry with two S and two N/O ligands. Phen probably removes the Ni from the Ni-labile form by binding to it as a bidentate chelate. The square-planar geometry of the nonlabile form suggests that phen cannot remove this Ni because its two open coordinate sites are trans to each other and inaccessible to phen. Phen may remove the Ni of the Ni-labile form because it has two open coordinate sites cis to each other. This proposed geometry is congruent with the function of the labile Ni as the methyl and CO binding site. Migratory insertion reactions generally occur with CO and methyl group bound at adjacent cis positions on a single metal ion.²³

Another difference between the Ni-labile and nonlabile forms is that only the former can be methylated. This process not only requires an open coordination site, but a surrogate $n = 2$ redox agent called the D site that provides the electrons needed to maintain the Ni in the 2+ state when it is methylated with " CH_3^+ ". Barondeau and Lindahl proposed that D is a low-potential cystine/cysteine pair, one sulfur of which is coordinated to the labile Ni in the oxidized disulfide form.²¹ Assuming that

the square-planar Ni in the nonlabile form has an open site available for methylation, the inability to methylate the nonlabile form may arise because the D site is absent or nonfunctional.

Removal of Ni by phen is inhibited in the presence of various low-potential reductants, including dithionite, CO, Ti(III) citrate, and reduced methyl viologen. All of these reductants are capable of reducing the D site, and none of them can reduce A_{ox} individually. One possibility is that when the D site is reduced, both cysteinates coordinate the labile Ni, rendering it 5-coordinate and resistant to chelation and removal by phen. The only problem with this idea is that DTT inhibits the reaction of phen and Ni, despite its inability to reduce D_{ox} .²¹ One of the thiol groups of DTT may bind the Ni and render it 5-coordinate even though D remains oxidized. This binding may be rather weak, in that 1 mM DTT does not completely inhibit removal of labile Ni by phen.

What might be the function of the Fe_4S_4 cube in catalysis? Since there appears to be intracuster electron transfer between the labile Ni and the cube, the cube may be an electron transfer conduit; it could promote electron transfer from the C-cluster to the D site, a redox step required to activate the A-cluster for catalysis. Alternatively (or additionally), the cube/bridge assembly may stabilize the labile Ni in a geometry conducive to binding, and eventually reacting, CO and the methyl group, and/or it may stabilize or activate the D site cysteines so that they function as required.

The proposed structures of the different A-cluster forms illustrated in Figure 8, and the possible functions of the Ni and the cube in catalysis just discussed, are useful because they are congruent with, and summarize, all available relevant experimental results. We are keenly aware that further tests are required before these proposed structures and functions can be considered established, and that the results of such tests may suggest modifications. Nevertheless, at present they provide an intellectual scaffold upon which such tests may be conceived, and we believe that they add new insight into the bioorganometallic mechanism of this unique enzyme.

Acknowledgment. Research in the P.A.L. lab is supported by the National Institutes of Health (Grant GM46441) and the Robert A. Welch Foundation (Grant A1170). XAS work in the R.A.S. laboratory is supported by the National Institutes of Health (Grant GM42025). C.M.V.S. collected and analyzed the XAS data, R.A.S. helped interpret the XAS data and provided intellectual input, W.K.R. and J.X. performed and analyzed the UV-vis, EPR, and inhibition experiments, and P.A.L. provided advice and oversight.

JA981165Z

(52) Collman, J. P.; Halbert, T. R.; Suslick, K. S. *Metal Ion Activation of Dioxygen*; J. Wiley: New York, 1980.